Study of the effects of cross section shape on the structural behaviour of helical wires on a bent flexible structure

Fang, Pan; Li, Xiao; Jiang, Xiaoli; Hopman, Hans; Bai, Yong

Publication date
2023

Document Version
Final published version

Published in
Proceedings of the Thirty-third (2023) International Ocean and Polar Engineering Conference

Citation (APA)
Fang, P., Li, X., Jiang, X., Hopman, H., & Bai, Y. (2023). Study of the effects of cross section shape on the structural behaviour of helical wires on a bent flexible structure. In J. S. Chung, D. Wan, S. Yamaguchi, & More Editors (Eds.), *Proceedings of the Thirty-third (2023) International Ocean and Polar Engineering Conference* (pp. 1725-1731). Article ISOPE-I-23-252 (Proceedings of the International Offshore and Polar Engineering Conference). International Society of Offshore and Polar Engineers (ISOPE).

Proceedings of the Thirty-third (2023) International Ocean and Polar Engineering Conference
Ottawa, Canada, June 19-23, 2023

ISBN 978-1-880653-80-7; ISSN 1098-6189
www.isope.org

Study of the effects of cross section shape on the structural behaviour of helical wires on a bent flexible structure

Pan Fang[a,*]*; Xiao Li*[b]*; Xiaoli Jiang*[a]*; Hans Hopman*[a]*; Yong Bai*[c]
[a]Department of Maritime and Transport Technology, Delft University of Technology, Netherlands
[b]Institute of High Performance Computing (IHPC), Agency for Science, Technology and Research (A*STAR), Singapore
[c]College of Civil Engineering and Architecture, Zhejiang University, Hangzhou, Zhejiang, P.R. China

ABSTRACT

Helical wires are a type of structure winding around on an underneath layer in flexible structures. They constitute a structure layer that provides mechanical protection and sufficient flexibility. The cross section of a helical wire could differ from round to rectangular. The curvature increments of a helical wire on a bent flexible structure can be influenced by the cross section shape due to the contact restriction from the neighbouring layer. The shape effect causes a different mechanical behaviour of the wire itself. However, this effect is not fully understood up till now. This paper mainly investigates the curvature increments of helical wires with rectangular and round cross section by using numerical method. This model takes advantage of the properties belonging to solid elements and beam elements by embedding the latter into the former. The solid element is able to retain the geometry detail of the cross section as much as possible in order to get deep insight of the shape effect. The beam element based on Timoshenko beam theory with well defined Frenet-Serret frames can accurately output the curvature increments in three local directions. Then widly-used analytical models are presented and deployed to verify the numerical results. The research results show the application condition of the analytical expressions and benefit the cable/umbilical/flexible pipe designers.

KEY WORDS: cross section shape; helical wires; flexible structures; curvature; FEM

INTRODUCTION

Helical wires have played a key role in flexible structures such as flexible pipes, umbilicals and submarine power cables(Sævik, 1992, Witz and Tan, 1995, Fang et al., 2021). They usually serve as a structural layer to protect the inner layers from mechanical failure and meanwhile provide certain flexible property so that the flexible structure is able to bend to an aimed curvature. Even though they have been widely and extensively used in flexible structures for a long history, and helical wires can also date back to helical ropes that tons of studies have been put into(Raoof and Kraincanic, 1995, Wang et al., 2015, de Menezes and Marczak, 2021), their structural behaviour is still not clear to engineers, especially when the flexible structure is under bending, due to not only their complex geometry configuration, but also the contact between them and their neighbouring layers.

In order to investigate the structural responses of helical wires, analytical method was firstly used and the analytical formulas have been evolved all the time. A systematic study about the helical wires used in helical ropes can be traced back to the literature(Costello, 1997). Differential geometry is the fundamental for the derivation of the constitutive equation of helical wires under different loadings. Frenet-Serret frames or Darboux Frames are defined on helical wires as local coordinate system so that the structural responses in the local frame can be obtained. As the analytical models simplify helical wires as beam element, they are unable to consider the effect of cross section shape. More specifically, for example, the contact situation between a helical wire and its neighbouring underneath layer is different for a cross section with rectangular and circular due to the cross section twist restriction from the rectangular. However, this difference is unable to be reflected by a beam wire. Therefore, for the case of a wire on an underneath layer, no matter it is a round or rectangular shape, the slip path of the wire is usually treated as two ways(Dai et al., 2017): the loxodromic and geodesic slip path. The former one assumes the wire sticks on its neighbouring layers during bending without transverse slip, thus could cause a curvature change in this direction. The geodesic slip path, instead, is defined as the shortest path between the intrados and extrados on the neighbouring cylinder, thus causing a transverse slip and there is no curvature change in this direction. Based on either one of the two assumptions regarding helical wires on the underneath layer, the kinematic configuration is determined. However, it is found in fact the slip path of a helical wire in the real situation is somewhere between loxodromic and geodesic path.

In order to consider the effect of cross section shape on the slip path, another popular approach that can be used to determine the structure behaviour of helical wires is numerical method. Although this method is not as efficient as analytical methods during the calculation process, it provides a good tool to capture the slip behaviour among the contact interfaces numerically without making assumption about the slip path. On the other hand, unlike that an analytical method is especially derived for helical wires with certain type of cross section, a numerical method can be used for helical wires with different types of cross section, requiring only a few revision to the numerical model. Many previous scholars have put much effort into the study of helical wires, no matter it is about all the helical wires on a full cross section(Lukassen et al., 2019), or a helical wire on the underneath

layer(Dong et al., 2019). In the open literature, the study is usually focused on helical wires with rectangular cross section because this type of cross section is more observed in flexible structures. However, there is also round cross section being used, especially in submarine power cables, and there is neither enough study about it nor comparison research about these two types of cross section shape. Therefore, the structural behaviour of these two types of cross section shape is not fully understood yet.
In this paper, finite element method (FEM) is used to deal with the mechanical behaviour of helical wires with rectangular and round cross section. Then the influence of cross section shape is discussed based on the obtained results. The obtained conclusions will benefit the practitioner and scholars who are studying the mechanical behaviour of flexible structures with helical wires.

FINITE ELEMENT MODEL

The aim of this paper is to study the mechanical behaviour of helical wires in a bent flexible structure. Due to the periodic behaviour of the helical wires, only a single wire is built with an underneath layer to facilitate the simulation process. The finite element simulation is performed with the software package ABAQUS(Abaqus, 2014) and the final model is shown in Fig. 1. Noteworthy there are three components in Fig. 1 whereas only two are observed. This is because a beam wire is embedded inside the solid helical wire. The beam wire has a very low Young's modulus, which contributes almost nothing to the structural response of the overall structure and only serves as a medium to output the curvature change of the solid helical wire.
The simulation includes two types of cross section shapes of the helical wire: rectangular and round. Their geometry parameters are given in Section 4 in detail. The radius of the helical wire cross section is determined according to the area equivalence to the rectangular wire.

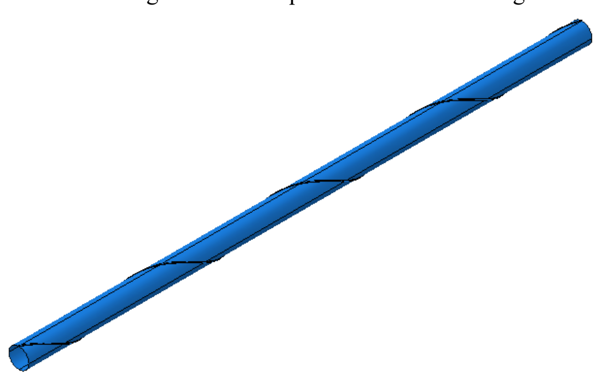

Fig. 1 The single wire finite element model

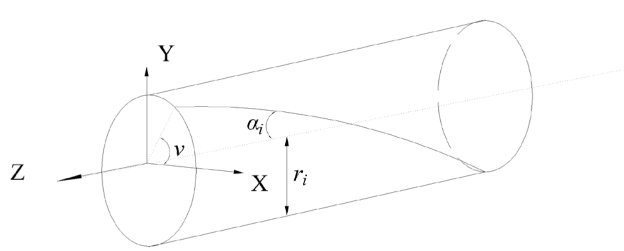

Fig. 2 Helical wire on a cylinder

Load and boundary conditions

In order to reach constant curvature over the structure, a set of reference points (RPs) are built on the centreline, as shown in Fig. 3. Each RP is coupled to its corresponding cross section by means of kinematic coupling constraints with regard to all the degree of freedoms (DOFs). In this way, the movements of each cross section are controlled through the RPs. Meantime, the cross section is restricted in the radial direction, which means there is no radial deformation and therefore is corresponding to the assumption in analytical models.
The cross section in the middle along the centreline is the symmetric plane of the structure when it is under bending, therefore, the RP in the middle is totally fixed to avoid rigid body motion. Since the bending is symmetric about the middle plane, only half of the structure is discussed here. Taking the right part as an example, except the RP in the middle, the other RPs are sorted into two types: master RP on the most right and slave RPs for the left, as shown in Fig. 4. The slave RPs move in certain rules according to the master RP.
Two steps are applied for the model: a tension step and a bending step. The followed tension forces are applied on the most left and most right RPs, as illustrated by Fig. 4. The DOFs of the master RP and slave RPs on the right side are given in Table 1. Notice there is a bending angle in the X direction and a displacement in the Y direction on the master RP, the movement of the slave RPs are obtained through nonlinear multi-point constraint MPC ABAQUS user subroutines. According to Diehl (Diehl, 1993) and Abaqus (Abaqus, 2014), for ABAQUS to process an user-defined MPC, three components are supposed to be supplied:
a. A matrix of DOF identifiers, JDOF(MDOF,N).
b. Matrices representing derivatives of the constraint function regarding the nodal DOFs.
c. The values of the dependent DOFs based on the independent DOF values.

Table 1 Boundary conditions of the right half-structure

	Master RP		Slave RPs	
	Step 1	Step 2	Step 1	Step 2
U1	0	0	0	0
U2	0	u_y^{M}	0	-
U3	-	-	-	-
UR1	0	φ_x^M	0	-
UR2	0	0	0	0
UR3	-	-	-	-

- 0 means the corresponding DOF is fixed, whereas – means the corresponding DOF is free. u_y^{M} and φ_x^M will be explained below.

In the case over here, U2 and UR1 of the slave RPs are determined by the master RP. At first, the bending radius can be expressed as:

$$F(x,y,z;t) = R_B = \frac{X_z^{\mathrm{M}} + u_z^{\mathrm{M}}}{\varphi_x^M} \tag{1}$$

Where X, u and φ are the initial coordinate, displacement and rotation angle, respectively. The superscript M denotes master RP while the subscripts mean the coordinate axes. Then the displacement of the master RP in the Y direction is:

$$f_1(u_y^{\mathrm{M}}, \varphi_x^{\mathrm{M}}) = u_y^{\mathrm{M}} - R_B(1 - \cos\varphi_x^{\mathrm{M}}) = 0 \tag{2}$$

Then the movement of the slave RPs can be calculated according to the maser RP's displacement and the movement of the RPs are:

$$\varphi_x^{\mathrm{S}} = \varphi_x^{\mathrm{M}} \frac{X_z^{\mathrm{S}}}{X_z^{\mathrm{M}}} \tag{3}$$

$$u_y^{\mathrm{S}} = R_B(1-\cos\varphi_x^{\mathrm{S}}) \tag{4}$$

$$u_z^{\mathrm{S}} = R\sin\varphi_x^{\mathrm{S}} + X_z^{\mathrm{S}} \tag{5}$$

Where the superscript S denotes the slave node. Again, Eq. (3), Eq. (4) and Eq. (5) can be rewritten according to the form of the user subroutine MPC:

$$f_1(\varphi_x^{\mathrm{S}}, \varphi_x^{\mathrm{M}}) = \varphi_x^{\mathrm{S}} - \varphi_x^{\mathrm{M}} \frac{X_z^{\mathrm{S}}}{X_z^{\mathrm{M}}} = 0 \tag{6}$$

$$f_2(u_y^{\mathrm{S}}, u_z^{\mathrm{M}}, \varphi_x^{\mathrm{M}}) = u_y^{\mathrm{S}} - R_B(1-\cos\varphi_x^{\mathrm{S}}) = 0 \tag{7}$$

$$f_3(u_z^{\mathrm{S}}, u_z^{\mathrm{M}}, \varphi_x^{\mathrm{M}}) = u_z^{\mathrm{S}} - R\sin\varphi_x^{\mathrm{S}} - X_z^{\mathrm{S}} = 0 \tag{8}$$

By inputting the partial derivatives of the constraint functions involving corresponding DOFs into the ABAQUS subroutine, a constant curvature can be achieved.

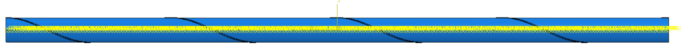

Fig. 3 Illustration of the RPs

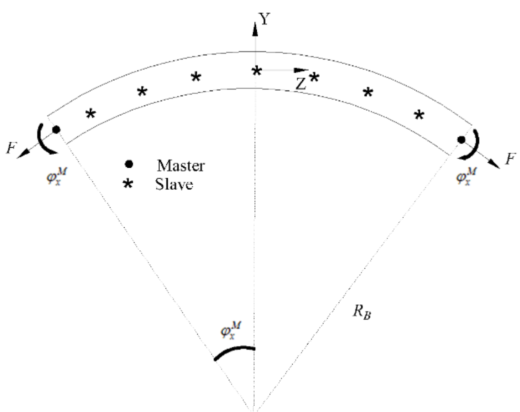

Fig. 4 Illustration of master and slave RPs

Mesh and interaction

The underneath core layer is simplified by using shell element in order to decrease the computation resource. Meantime, radial deformation is disregarded in analytical models and shell element in FEM significantly decrease the effect of radial deformation of the underneath layer. Then solid element and beam element are selected for the solid helical wire and beam helical wire, respectively. The final mesh of the structure is shown in Fig. 5 where there are in total 250 elements along the pipe axial direction. An 8-node linear brick, reduced integration, hourglass control (C3D8R) element is assigned for the solid wire, A 2-node linear beam in space (B31) element based on Timoshenko beam theory is assigned for the beam wire and A 4-node doubly curved thin or thick shell, reduced integration, hourglass control, finite membrane strains (S4R) element is assigned for the underneath core. Local coordinate frame is assigned on the beam wire, as illustrated in Fig. 6 where 1 is the normal direction, 2 the transverse direction and 3 the torsion direction.

The interaction between the underneath layer and the solid wire is simulated as surface-to-surface contact with a contact stiffness of 2000 N/mm^3 (Lukassen et al., 2019) and a friction coefficient of 0.2. In addition, the beam wire is put along the centre point of all the cross sections of the solid wire and tied together with the solid wire so that it can output the curvature change of the wire.

Dynamic implicit algorithm is applied in the simulation and after the calculation, the energy ratio between Kinetic Energy for Whole Model (ALLKE) and Total Strain Energy for Whole Model (ALLSE) need to be checked before analyzing the results since a quasi-static status should be obtained. As a general rule, ALLKE should range in a small fraction(typically 5% to 10%) of ALLIE throughout most of the process (Abaqus, 2014).

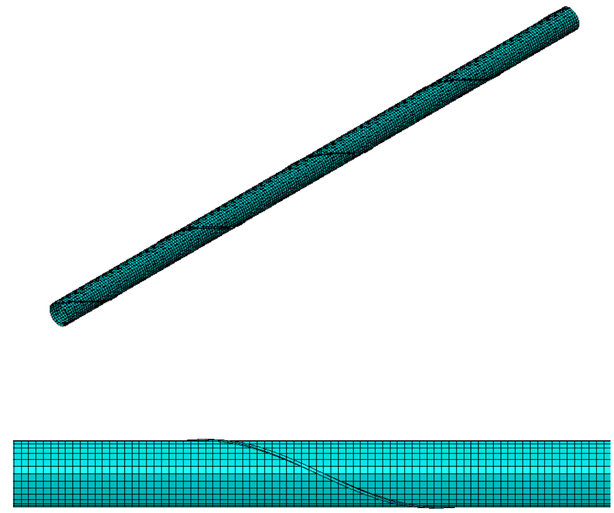

Fig. 5 Mesh of the structure

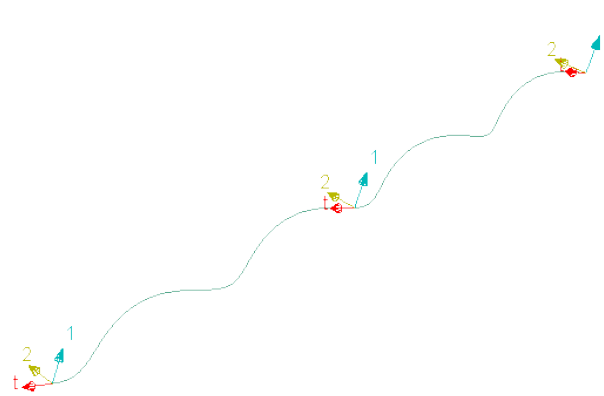

Fig. 6 Local coordinate frame for the beam wire

ANALYTICAL MODEL

The analytical model is used to predict the curvature increment of helical wires on a bent structure, and then the results are used to verify the numerical results. (Dong et al., 2019) derive general expressions based on the generalized Frenet-Serret equations and then degenerate them to the same expressions given by the previous scholars by ignoring a few high-order items. Four of the most common equations for the curvatures in the three directions are summarized as follows:

Analytical model 1: (LeClair and Costello, 1988)

$$\Delta\kappa_1 = \kappa\sin\alpha_0\cos\alpha_0\cos\theta \tag{9}$$

$$\Delta\kappa_2 = \kappa \sin\alpha_0 \sin\theta \tag{10}$$

$$\Delta\kappa_3 = \kappa \cos^2\alpha_0 \cos\theta \tag{11}$$

Analytical model 2: (Sathikh, 1990, Huang and Vinogradov, 1994)

$$\Delta\kappa_1 = \kappa \sin\alpha_0 \cos\alpha_0 \cos\theta \tag{12}$$

$$\Delta\kappa_2 = \kappa \sin^2\alpha_0 \cos\alpha_0 \sin\theta \tag{13}$$

$$\Delta\kappa_3 = \kappa \cos^2\alpha_0 \cos\theta \tag{14}$$

Analytical model 3: (Sævik, 1993, Sævik, 2011, Sævik, 1992, Sathikh et al., 2000, Skeie et al., 2012)

$$\Delta\kappa_1 = \kappa \sin\alpha_0 \cos^3\alpha_0 \cos\theta \tag{15}$$

$$\Delta\kappa_2 = \kappa(1+\sin^2\alpha_0)\cos\alpha_0 \sin\theta \tag{16}$$

$$\Delta\kappa_3 = \kappa \cos^4\alpha_0 \cos\theta \tag{17}$$

Analytical model 4: (Pesce et al., 2010, Sævik and Li, 2013)

$$\Delta\kappa_1 = 2\kappa \sin\alpha_0 \cos^3\alpha_0 \cos\theta \tag{18}$$

$$\Delta\kappa_2 = \kappa(1+\sin^2\alpha_0)\cos\alpha_0 \sin\theta \tag{19}$$

$$\Delta\kappa_3 = \kappa \cos^2\alpha_0 \cos 2\alpha_0 \cos\theta \tag{20}$$

It can be observed from the above expressions that the parameters influencing the curvature change $\Delta\kappa_1$, $\Delta\kappa_2$ and $\Delta\kappa_3$ in three directions include pipe bending curvature κ, the winding angle α_0 and the angle θ used to represent the wire location, as shown in Fig. 2. The fourth classical analytical models will be used to compare with the FE results.

CASE STUDY

Sections 2 and Section 3 discusses FE model and presents the classical analytical models, respectively. This part will use the FE model and analytical models to investigate the difference of helical wires with rectangular and round cross sections.

Cross section and material properties

For the case study here, there are two types of cross section shapes: rectangular and round, as shown in Fig. 7. The magnitudes of the areas of these two types of cross section are the same. The rectangular cross section has a thickness of 5 mm and width of 12.5 mm. The round cross section has a diameter of 8.92 mm and the other parameters are the same as the rectangular wire. The length of the model is 7144 mm, the length of four pitches. The material properties of the three components constituting the structure are listed in Table 2. Totally, 8 cases are studied in this paper in which Case 1-4 are for rectangular helical wire and Case 5-8 are for round helical wire. They are given in detail in Table 3. Again, the tension load is applied at first before the bending. A curvature of 6e-3/m is applied on the flexible structure. This is realized by applying corresponding angle φ_x^M and displacement u_y^M on the master reference point, like the boundary condition in Table 1.

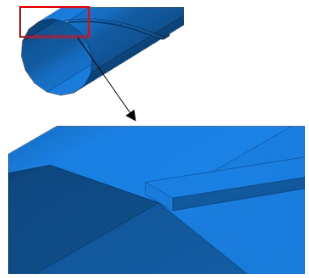

(a)

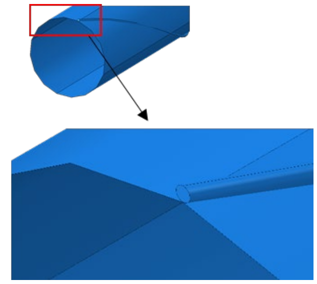

(b)

Fig. 7 Model with rectangular (a) and round (b) wire cross section

Table 2 Geometry information of the simulation structure with rectangular wire

Component	Geometry	Outer diameter (mm)	Materials
Underneath layer	Thickness = 0.1mm	258	E = 2.1e5 MPa Poisson's ratio = 0.35
Solid wire	Winding angle = 24.8 deg	268	E = 2.1e5 MPa Poisson's ratio = 0.3
Beam wire	Circular cross section (r = 0.1 mm)	263	E = 10 MPa Poisson's ratio = 0.3

Table 3 Details of the 8 cases

Cases No.	Case description (Unit: N)
Case 1	Round, tension = 0
Case 2	Round, tension = 50
Case 3	Round, tension = 500
Case 4	Round, tension = 5000
Case 5	Rectangular, tension = 0
Case 6	Rectangular, tension = 50
Case 7	Rectangular, tension = 500
Case 8	Rectangular, tension = 5000

Results and Discussions

The curvature increments in three directions along with the wire distance regarding Case 1 to Case 4 are shown in Fig. 8-10. Noteworthy, only one pitch of the helical wire in the middle along the axis of the structure is picked up to generate the curvature increment in order to get rid of the boundary effect. It can be observed that the curvatures in the three directions overlap with each other quite well no matter how much the tension is applied, and the curves are symmetric about the horizontal 0 axis, which means the curvature increment is symmetric about the bending plane. This is due to the free movement of the round cross section where there is no redundant contact restriction in the torsion direction.

The comparisons of the three curvature increments of the analytical model 4 and FEM results are shown in Fig. 11-13. The agreement between these two methods regarding the round shape wire are quite good in general. The largest differences between the analytical model and the FE model appear at the extrados and the intrados, i.e., where v = 180 deg and v = 360 deg, respectively. This area contains the highest error of normal curvature of 19%. The given analytical model is found to be able to predict the curvature increment of most wire area for round helical wire.

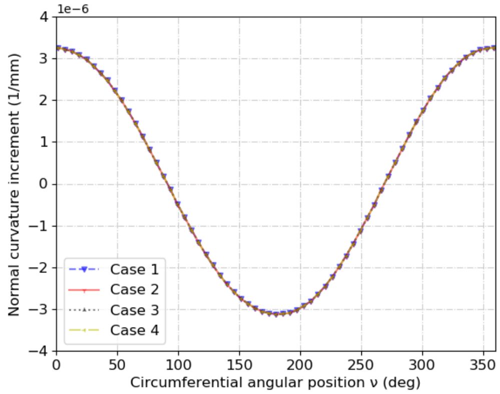

Fig. 8 Normal curvature increment along with the circumferential wire location

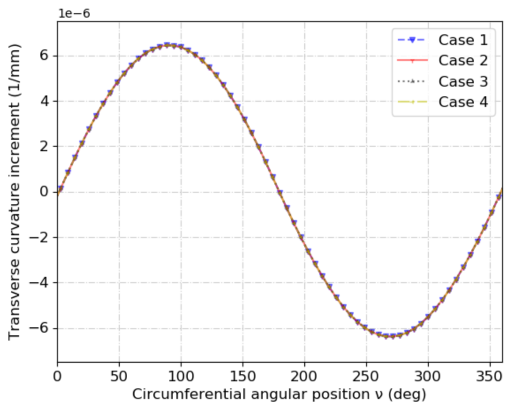

Fig. 9 Transverse curvature increment along with the circumferential wire location

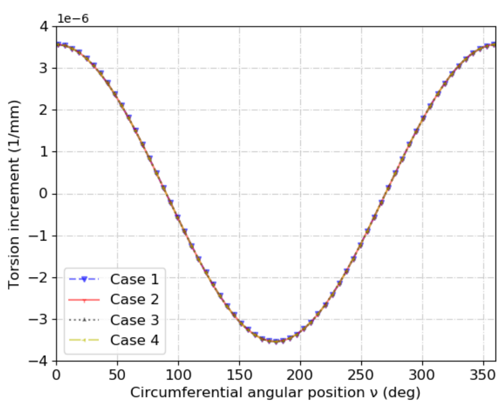

Fig. 10 Torsion increment along with the circumferential wire location

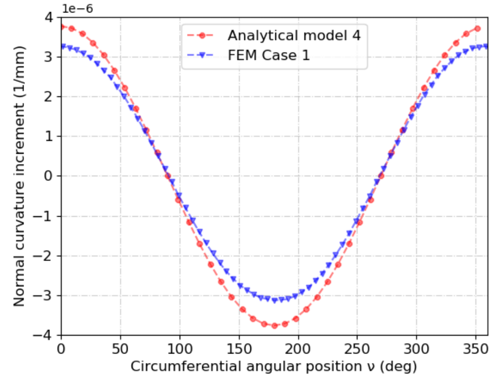

Fig. 11 Normal curvature increment for the round wire under analytical model and FE model

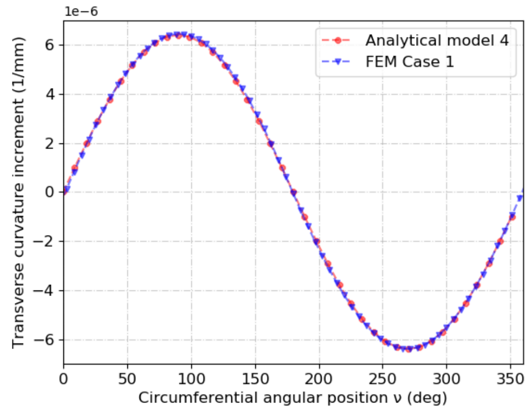

Fig. 12 Transverse curvature increment for the round wire under analytical model and FE model

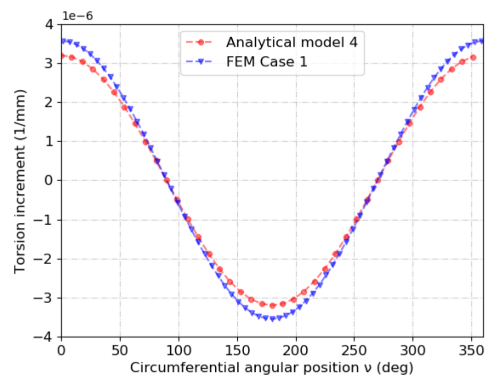

Fig. 13 Torsion increment for the round wire under analytical model and FE model

The curvature increments for the rectangular shape wire, i.e., Case 5 to Case 8, are given in Fig. 14-16. It can be observed from the three images that, unlike the round shape wire, normal curvature increment and torsion curvature increment of the rectangular shape wire are affected much by the tension. There is an error near 13% and 114% for these two curvatures when the wire is located at the extrados. The transverse curvature increment, on the contrary, is hardly affected by the applied tension. When the tension force is less equal to 500 N, the curves basically symmetric about the 0 horizontal axis, illustrating the curvature change is symmetric about the bending plane. However, when the tension is increased to 5000 N, the wire near the extrados has higher absolute value regarding the normal curvature and torsion curvature.

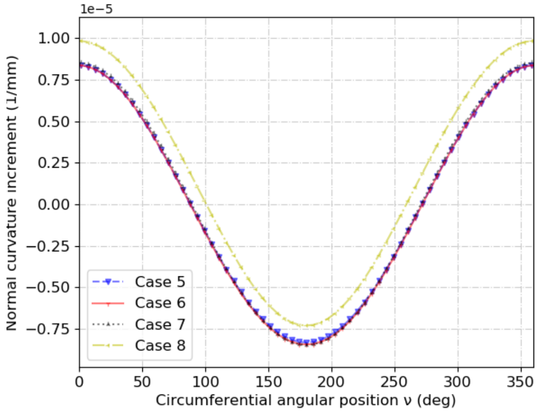

Fig. 14 Normal curvature increment along with the circumferential wire location

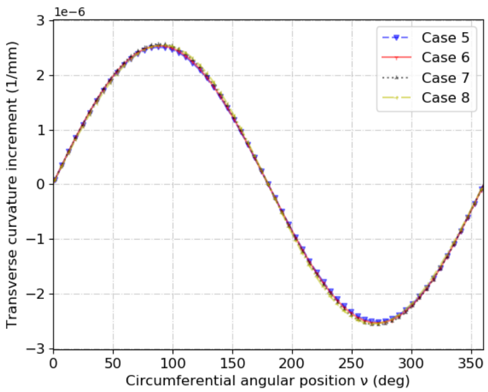

Fig. 15 Transverse curvature increment along with the circumferential wire location

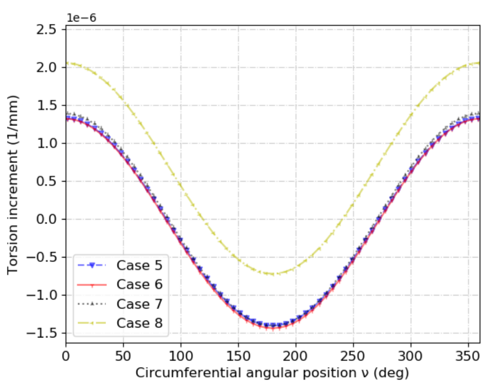

Fig. 16 Torsion increment along with the circumferential wire location

The curvatures from Case 5 are also extracted out to compare with the analytical model 4. They are shown in Fig. 17-19. It can be observed that there is a big discrepancy regarding the three curvatures from the analytical and FE models. The reason could be caused by the cross section of the rectangular wire that restrict the rotation around its own axis. This restriction makes the torsion increment much less than that predicted by the analytical model. Meanwhile, rectangular is not able to move transversely totally free. This also causes the transverse curvature from the FE model less than that from the analytical model. On the other hand, the normal curvature increment from FE model is observed to be higher than that in the analytical model. The results show that cross section shape of a wire needs to be carefully considered while doing the analytical study. The derivation of analytical models in the previous study did not consider this point, causing the difference between the analytical model and FE model.

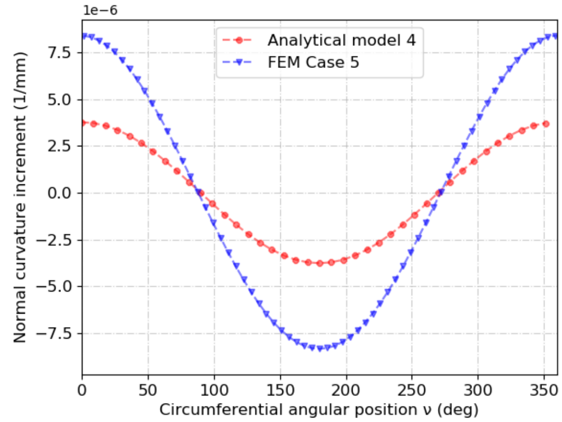

Fig. 17 Normal curvature increment for the rectangular wire under analytical model and FE model

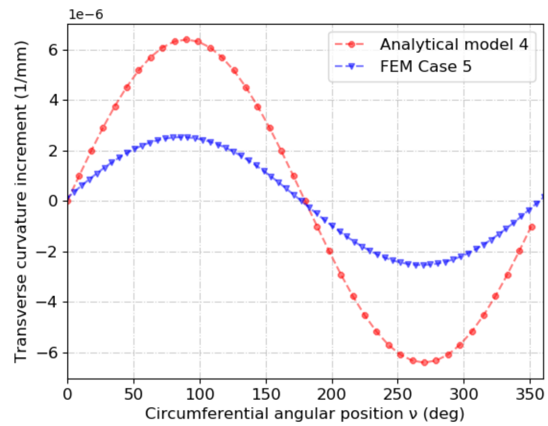

Fig. 18 Transverse curvature increment for the rectangular wire under analytical model and FE model

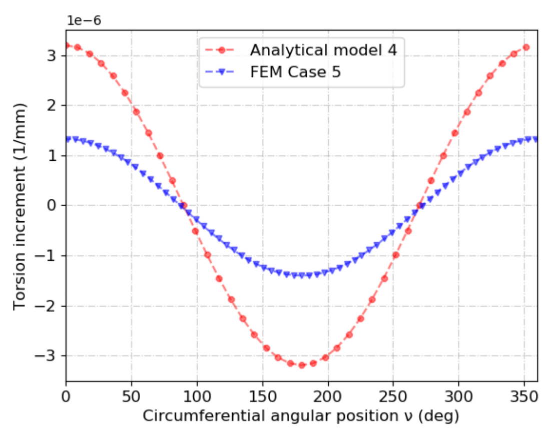

Fig. 19 Torsion increment for the rectangular wire under analytical model and FE model

CONCLUSIONS

In this study, an FE model under constant bending curvature is proposed to study the cross section shape effect on the structural behavior of a wire. The FE model takes advantage of the solid element that can represent the geometry detail, and meanwhile exploits the beam element with well defined Frenet-Serret frames that is able to output the curvature increments in local directions. The differences of helical wires between rectangular and round cross sections are studied and discussed. A few findings are concluded below:

1) The normal and torsion curvatures of wires with rectangular cross section can be affected by tension, with a largest error of 114%, while the counterparts of wire with round cross section are hardly affected by tension.
2) Tension force can cause the curvature unsymmetrical about the neutral plane of the flexible structure. The value in the tension part is higher than that in the compressive part.
3) The previous analytical models can be applied on the helical wires with round cross section, causing acceptable error in most of the wire area. However, the analytical models do not fit the helical wires with rectangular cross section. There could be a three times of difference between the analytical and numerical results. This could be caused by the slip assumptions during analytical derivation.

Helical wires as key components inside flexible structures protect the inner layers and provide enough flexibility, their mechanical behaviour always attracts much attention. This paper probes into the difference of helical wires with different cross section and discovers that previous analytical expressions might not be able to predict the curvature change of helical wire with rectangular cross section appropriately. Numerical method using solid elements that considers the geometry detail of a wire is highly recommended during the prediction. Practitioners and engineers should be more cautious when the analytical expressions are applied to predict the curvature increment.

ACKNOWLEDGEMENTS

The first author Pan Fang was supported by the China Scholarship Council [grant number 201906320047].

REFERENCES

ABAQUS, V. 2014. 6.14 Documentation. *Dassault Systemes Simulia Corporation,* 651**,** 6.2.

COSTELLO, G. A. 1997. *Theory of wire rope*, Springer Science & Business Media.

DAI, T., SÆVIK, S. & YE, N. 2017. Friction models for evaluating dynamic stresses in non-bonded flexible risers. *Marine Structures,* 55**,** 137-161.

DE MENEZES, E. A. & MARCZAK, R. J. 2021. Comparative analysis of different approaches for computing axial, torsional and bending stiffnesses of cables and wire ropes. *Engineering Structures,* 241**,** 112487.

DIEHL, T. 1993. Formulation of a User MPC to Simulate Beam-Type Transport Problems. MFSP Internal Report, Department of Mechanical Engineering, University of….

DONG, L., QU, Z., ZHANG, Q., HUANG, Y. & LIU, G. 2019. A general model to predict torsion and curvature increments of tensile armors in unbonded flexible pipes. *Marine Structures,* 67**,** 102632.

FANG, P., JIANG, X., HOPMAN, H. & BAI, Y. 2021. Mechanical responses of submarine power cables subject to axisymmetric loadings. *Ocean Engineering,* 239**,** 109847.

HUANG, X. & VINOGRADOV, O. 1994. Analysis of dry friction hysteresis in a cable under uniform bending. *Structural Engineering and Mechanics,* 2**,** 63-80.

LECLAIR, R. & COSTELLO, G. 1988. Axial, bending and torsional loading of a strand with friction.

LUKASSEN, T. V., GUNNARSSON, E., KRENK, S., GLEJBØL, K., LYCKEGAARD, A. & BERGGREEN, C. 2019. Tension-bending analysis of flexible pipe by a repeated unit cell finite element model. *Marine Structures,* 64**,** 401-420.

PESCE, C. P., RAMOS JR, R., DA SILVEIRA, L. M. Y., TANAKA, R. L., MARTINS, C. V. D. A., TAKAFUJI, F. C. M., NOVAES, J. O. P. Z. L. & GODINHO, C. A. F. Structural behavior of umbilicals: part I—mathematical modeling. International Conference on Offshore Mechanics and Arctic Engineering, 2010. 871-880.

RAOOF, M. & KRAINCANIC, I. 1995. Analysis of large diameter steel ropes. *Journal of engineering mechanics,* 121**,** 667-675.

SÆVIK, S. 1992. On stresses and fatigue in flexible pipes.

SÆVIK, S. 1993. A finite element model for predicting stresses and slip in flexible pipe armouring tendons. *Computers & structures,* 46**,** 219-230.

SÆVIK, S. 2011. Theoretical and experimental studies of stresses in flexible pipes. *Computers & Structures,* 89**,** 2273-2291.

SÆVIK, S. & LI, H. Shear interaction and transverse buckling of tensile armours in flexible pipes. International Conference on Offshore Mechanics and Arctic Engineering, 2013. American Society of Mechanical Engineers, V04AT04A013.

SATHIKH, S. 1990. Discussion:"Axial, Bending and Torsional Loading of a Strand With Friction"(LeClair, RA, and Costello, GA, 1988, ASME J. Offshore Mech. Arct. Eng., 110, pp. 38–42).

SATHIKH, S., RAJASEKARAN, S., JAYAKUMAR & JEBARAJ, C. 2000. General thin rod model for preslip bending response of strand. *Journal of engineering mechanics,* 126**,** 132-139.

SKEIE, G., SØDAHL, N. & STEINKJER, O. 2012. Efficient fatigue analysis of helix elements in umbilicals and flexible risers: Theory and applications. *Journal of Applied Mathematics,* 2012.

WANG, X.-Y., MENG, X.-B., WANG, J.-X., SUN, Y.-H. & GAO, K. 2015. Mathematical modeling and geometric analysis for wire rope strands. *Applied Mathematical Modelling,* 39**,** 1019-1032.

WITZ, J. & TAN, Z. 1995. Rotary bending of marine cables and umbilicals. *Engineering structures,* 17**,** 267-275.